Title: Dual Effects of Gossypol on Human Hepatocellular Carcinoma via Endoplasmic Reticulum Stress and Autophagy

Authors: Guang Zhang, Zhongxia Wang, Weibo Chen, Yin Cao, Junyi Wu, Guanghui Qiang, Anlai Ji, Junhua Wu, Chunping Jiang

PII: S1357-2725(19)30106-2
DOI: https://doi.org/10.1016/j.biocel.2019.05.012
Reference: BC 5543

To appear in: *The International Journal of Biochemistry & Cell Biology*

Received date: 18 February 2019
Revised date: 19 May 2019
Accepted date: 21 May 2019

Please cite this article as: Zhang G, Wang Z, Chen W, Cao Y, Wu J, Qiang G, Ji A, Wu J, Jiang C, Dual Effects of Gossypol on Human Hepatocellular Carcinoma via Endoplasmic Reticulum Stress and Autophagy, *International Journal of Biochemistry and Cell Biology* (2019), https://doi.org/10.1016/j.biocel.2019.05.012

Dual Effects of Gossypol on Human Hepatocellular Carcinoma via Endoplasmic Reticulum Stress and Autophagy

Guang Zhang[1, *], Zhongxia Wang[1, *], Weibo Chen[2], Yin Cao[1], Junyi Wu[1], Guanghui Qiang[3], Anlai Ji[4], Junhua Wu[5], and Chunping Jiang[1]

[1] Department of Hepatobiliary Surgery, the Affiliated Drum Tower Hospital of Nanjing University Medical School, Nanjing, Jiangsu 210008, China

[2] Department of Hepatobiliary Surgery, Changzhou First People's Hospital, the Third Affiliated Hospital of Soochow University, Changzhou, Jiangsu 213003, China

[3] Department of Hepatobiliary Surgery, Nanjing Drum Tower Hospital Clinical College of Nanjing Medical University, Nanjing, Jiangsu 210008, China

[4] Department of General Surgery, the Affiliated Hospital of Yangzhou University, 365 Hanjiang Middle Road, Yangzhou, Jiangsu 225000, China.

[5] Jiangsu Key Laboratory of Molecular Medicine, Medical School, Nanjing University, Nanjing, Jiangsu 210093, China

*These authors contributed equally to this work

Correspondence to: Chunping Jiang. Address: 321 Zhongshan Road, Nanjing, Jiangsu 210008, China. Telephone: +86-13851818663. Fax: +86-25-83307115. Email: chunpingjiang@163.com.
Junhua Wu. Address: 22 Hankou Road, Nanjing, Jiangsu 210008, China. Telephone: +86-13770920883. Fax: +86-25-83307115. Email: wujunhua@nju.edu.cn.

Word Count of text: 5028 words excluding references

Abstract

Treatment outcomes for hepatocellular carcinoma (HCC) remain unsatisfactory, and effective new therapeutic methods are urgently needed. Gossypol has been shown to have an anti-HCC effect, but the underlying mechanism requires further study. In this study, we found gossypol inhibited HCC cells in vitro and in vivo. Typical apoptosis was induced in HCC cells. Dilated ER and autophagosomes were observed by electron microscopy, and the activation of the unfolded protein response and autophagy markers suggested that gossypol induced both ER stress and autophagy. C/EBP homologous protein was the key factor that led to apoptotic cell death, whereas inositol-requiring enzyme 1α and eukaryotic initiation factor 2α played a protective role. Autophagy protected the cells from ER stress-related apoptosis. Both in vitro and in vivo studies indicated that inhibition of autophagy enhanced the anti-HCC effect of gossypol. Taken together, ER stress is the molecular mechanism underlying gossypol-induced apoptosis and autophagy. Gossypol exhibits anti-HCC activity primarily through the activation of apoptosis. However, gossypol-induced autophagy protects HCC cells from ER stress. Therefore, a combination therapy of gossypol and autophagy inhibitors may lead to an enhanced anti-HCC effect.

Abbreviations: HCC, hepatocellular carcinoma; ER, endoplasmic reticulum; UPR, unfolded protein response; IRE-1α, inositol-requiring enzyme 1 alpha; CHOP, C/EBP homologous protein; CQ, Chloroquine; eIF2α, eukaryotic initiation factor 2α; CCK-8, Cell Counting Kit-8; OD, optical density; PI, propidium iodide; TEM, Transmission electron microscopy; IHC, immunohistochemistry; TUNEL, Terminal Deoxynucleotidyl Transferase dUTP Nick End Labeling; PARP, poly ADP ribose polymerase; NC, negative control; BiP, binding immunoglobulin protein.

Keywords: hepatocellular carcinoma, gossypol, apoptosis, endoplasmic reticulum stress, autophagy

Introduction

Hepatocellular carcinoma (HCC) is the fifth most common cancer worldwide and the second most frequent cause of cancer-related death every year [1]. Despite improvements in treatment strategies for HCC over the last two decades, the outcome of this fatal disease remains unsatisfactory, as the 5-year survival rate is still below 20% [2]. In contrast to most other cancers, HCC does not involve the activation of a specific target, and most targeted drugs are thus ineffective [3]. Meanwhile, systemic therapy has been shown to be ineffective for patients with HCC [4]. The above-mentioned factors account for the challenges in HCC treatment.

Most anticancer agents kill cancer cells by inducing apoptosis [5], and enhanced endoplasmic reticulum (ER) stress is closely related to intrinsic apoptotic pathways [6, 7]. The ER is an organelle that is responsible for protein folding and Ca^{2+} storage [8], and ER stress appears when cells are exposed to specific pathological or physiological conditions. When cells are stressed, the unfolded protein response (UPR) is activated primarily through its sensors, such as PKR-like ER kinase, inositol-requiring enzyme 1 alpha (IRE-1α), and activating transcription factor, to restore ER homeostasis [9]. If ER homeostasis cannot be restored by the UPR, ER stress can lead to cell death, which is typically mediated by C/EBP homologous protein (CHOP), a proapoptotic transcription factor [10]. ER stress is always accompanied by autophagy, although the relationship between autophagy and apoptosis, which can be triggered by ER stress, remains controversial [11, 12]. Our previous study revealed that autophagy protects cells from apoptosis during ER stress [13]. Hence, we hypothesized that autophagic interference might sensitize cells to ER stress-induced apoptosis.

Gossypol is a component of cottonseed extract and is used as a fertility control agent due to its toxicity to sperm [14]. Recently, gossypol has been shown to possess anticancer effects against several cancer cell lines, including HCC cells [15-17]. In fact, gossypol is now in phase II/III clinical trials for various cancers. Previous studies have revealed that gossypol inhibits cancer cell proliferation or kills cancer cells by modulating a variety of signaling pathways [18-20]. Teng et al. found that gossypol induces DNA fragmentation by inhibiting protein kinase C activity [21]. Bcl-2 and Bcl-XL are the most studied targets of gossypol and are also closely related to cell proliferation. In a study by Baoleri et al., gossypol was found to down-regulate Bcl-2 protein expression, which further enhanced doxorubicin-induced apoptosis in cancer cells [17]. At the same time, gossypol also induces autophagy in cancer cells [22]. However, the specific role of gossypol-induced autophagy remains controversial. Gao et al. found that gossypol induces autophagy to protect cells from apoptosis, whereas Jang and Lee reported that gossypol causes autophagic cell death [23, 24]. In the present study, we further assessed the anticancer effects of gossypol against HCC cells. Our study also examined the novel role of ER stress and autophagy in gossypol-induced HCC cell apoptosis.

Materials and Methods

Cell culture and reagents. The human HCC cell lines PLC, Hep3B and Huh7 were purchased from the Cell Bank of the Chinese Academy of Sciences (Shanghai, China). The cells were cultured in Dulbecco's modified Eagle's medium (GIBCO BRL, Gaithersburg, MD) supplemented with 10% fetal bovine serum (GIBCO BRL, Gaithersburg, MD) and 100 U/mL penicillin and streptomycin. Both cell lines were maintained in a 5% CO_2 atmosphere at 37℃. Gossypol was purchased from Selleckchem (Houston, TX). Chloroquine (CQ) was obtained from Sigma-Aldrich

(St. Louis, MO). Annexin V-FITC kits and Fluo-3 AM were from the Beyotime Institute of Biotechnology (Nantong, China). Cell Counting Kit-8 (CCK-8) was obtained from Dojindo Laboratories (Kumamoto, Japan). An anti-LC3 (#L8918) rabbit antibody was purchased from Sigma-Aldrich (St. Louis, MO), and all other antibodies, anti-caspase-3 (#14220), anti-cleaved caspase-3 (#9664), anti-PARP (#9542), anti-cleaved PARP (#5625), anti-capase-9 (#9508), anti-cleaved caspase-9 (#52873), anti-CHOP (#2895), anti-BiP (#3177), anti-IRE-1α (#3294), anti-eIF2α (#5234), anti-phosphorylated eIF2α (#3597), anti-Atg-5 (#2630), anti-GAPDH (#5174), were from Cell Signaling Technology (Beverly, MA). For dilution rate: anti-LC3 and GAPDH was 1:3000, anti-Atg-5 was 1:1000, secondary antibodies were 1:10000, and the rest of antibodies were 1:500.

CCK-8 assay. Cell viability was determined using the CCK-8 assay. Briefly, 5.0×10^3 cells were grown on 96-well plates. After 24 h, the indicated dose of gossypol was added. The dilution vehicle was administered to the control group. After 48 h of incubation, the medium and gossypol were removed, and 100 μL CCK-8 working solution was added to each well. After 4 h of incubation, optical density (OD) was detected at 450 nm using a spectrophotometer (Molecular Devices Corporation, Sunnyvale, CA). The following formula was used to measure relative cell viability (%): OD (gossypol group) / OD (control group) × 100%.

Colony forming assay. A total of 500 cells were seeded in 6-well plates in culture medium. After 24 h, the indicated dose of gossypol was added, and the cells were further incubated with gossypol for 48 h. The medium and gossypol were then removed, and fresh culture medium was added. Colonies were grown for 20 days, and the medium was changed every week. The cells were stained with 0.1% crystal violet for 30 min after fixation with 3% paraformaldehyde for 20 min. The cells were washed with phosphate-buffered saline (PBS) three times and dried. Images were acquired with a digital camera, and colonies were counted using ImageJ software (National Institutes of Health, Bethesda, MD).

Western blot analysis. Cell lysates were prepared with RIPA lysis buffer (Beyotime, Nantong, China) according to the manufacturer's instructions. Total protein concentration was determined using a Bicinchoninic Acid Protein Assay Kit (Beyotime, Nantong, China) according to the manufacturer's instructions. In total, 20 μg protein was loaded onto each lane for electrophoresis with homogeneous SDS polyacrylamide gel (4% stacking gel, 10% or 12% separating gel depending on the molecular weight of target protein). Protein was electrophoresed in stacking gel under 60 voltage for 30 min and then electrophoresed under 100-110 voltage until fully separated. Then, the separated proteins were transferred to 0.45 μm polyvinylidene fluoride membranes (Millipore, Bedford, MA) by semi-dry transfer (50-80 mA per gel for 1 h). The membranes were incubated with the primary antibodies at 4℃ overnight followed by incubation with horseradish peroxidase-conjugated secondary antibodies at room temperature. The bands were visualized using a Tanon 5200 system (Beijing, China) after the addition of an enhanced chemiluminescence reagent (Millipore, Bedford, MA).

Measurement of intracellular calcium concentration. After the cells were treated with the indicated concentrations of gossypol for 48 h, they were incubated with 5 μM Fluo-3 AM calcium

probe for 1 h. The cells were then washed with PBS and placed in a 37℃ incubator for another 30 min to ensure that Fluo-3 was converted into fluorescent Fluo-3. Fluo-3 was detected using a FACSCalibur flow cytometer (BD Biosciences, San Jose, CA) following the manufacturer's instructions.

Small interfering RNA (siRNA) transfection. siRNAs against human CHOP and ATG5 were produced by GenePharma (Shanghai, China). The sequences of the siRNAs were as follows: si-ATG5, GGGAAGCAGAACCAUACUATT; and si-CHOP, AAGAACCAGCAGAGGUCACAA. si-IRE-1α and si-eIF2α was purchased from Santa Cruz Biotechnology (sc-40705 and sc-35273, Santa Cruz, CA). Scrambled siRNA was used as negative control (NC) in this study. The siRNA transfection protocol was described in our previous study [13].

Annexin V-FITC/propidium iodide (PI) staining. Cell aggregates were collected after treatment with different concentrations of gossypol for 48 h. The cells were resuspended with binding buffer, and annexin V-FITC was added. After incubation for 30 min, the cells were washed with PBS and incubated with PI for 20 min. Data were analyzed with FlowJo software after detection using a FACSCalibur flow cytometer (BD Biosciences, San Jose, CA).

Transmission electron microscopy (TEM). Cells treated with gossypol were collected and fixed in 4% glutaraldehyde. Ultrathin sections were obtained following published protocols [24], and the ultrastructures were observed with TEM (JEM-1010; JEOL, Tokyo, Japan).

HCC orthotopic xenograft assay. BALB/c nude mice were purchased from the College of Veterinary Medicine at Yangzhou University and raised according to the facility's protocol at the Animal Experiment Center of Drum Tower Hospital. The experimental protocol was reviewed by the local ethics committee. Generally, the mice were divided into four groups: control, gossypol, CQ, and gossypol+CQ groups. A total of 1.0×10^6 PLC cells were inoculated into the liver, and the mice were maintained for 1 week; then, the indicated drugs were administered by gavage. The mice were sacrificed after 4 weeks, and the liver, lung, heart, kidney, and spleen were collected.

Histological examinations and immunohistochemistry (IHC). Tissues fixed with 4% paraformaldehyde were embedded in paraffin and cut into 5-μm thick slices. For hematoxylin and eosin (H&E) staining, briefly, the tissue slices were dewaxed in xylene, rehydrated through decreasing concentrations of ethanol, and washed in PBS. Then the slices were stained with hematoxylin for 30 sec with agitation and rinsed in water. After that, the slices were stained with eosin for 10-30 sec with agitation and rinsed in water. After the staining, slices were dehydrated, mounted and covered with coverslip. IHC was carried out according to published protocols [25]. A rabbit anti-Ki67 monoclonal antibody (1:900, ab16667; Abcam, Cambridge, MA), rabbit anti-CHOP monoclonal antibody (1:100, 2895; Cell Signaling Technology, Beverly, MA), and a Colorimetric Terminal Deoxynucleotidyl Transferase dUTP Nick End Labeling (TUNEL) Apoptosis Assay Kit (C1091; Beyotime, Nantong, China) were used. The slices were observed and photographed using a microscope (BX50; Olympus, Tokyo, Japan).

Isolation of primary hepatocytes from mice

Primary hepatocytes were isolated from 12 to 14-week-old C57BL/6J mice. Firstly, the mice liver was perfused through portal vein with HANKS solution containing 0.5 mmol/L EDTA at a flow rate of 8 ml/min for 4 min and then perfused with HANKS solution containing 84 U/mL collagenase II, 10 mmol/L Hepes and 1.8 mM $CaCl_2$ for 6 min. The liver was dissected after removal, and then cells were separated from the debris with a 100μm BD filter. At last, cell suspension was centrifugated at 50 g for 3 min at 4℃ to collect hepatocytes. Isolated hepatocytes were seeded in culture plates coated with type I collagen and cultured in low glucose Dulbecco's modified Eagle's medium (GIBCO BRL, Gaithersburg, MD) supplemented with 10% fetal bovine serum (GIBCO BRL, Gaithersburg, MD) and 100 U/mL penicillin and streptomycin at 37℃ in an incubator supplemented with 5% CO_2 under humidified condition. After the cells attached to the dishes, the medium was replaced with serum-free low glucose Dulbecco's modified Eagle's medium.

Statistical analysis. Statistical analyses were performed with IBM SPSS software. Data are expressed as the mean ± standard deviation (SD). The means were compared using the unpaired, two-tailed Student's t-test or one-way analysis of variance for multiple comparisons. $P < 0.05$ was considered statistically significant.

Results

Gossypol induces apoptosis in HCC cells. We first studied the anti-HCC effect of gossypol in two human HCC cell lines, PLC/PRF/5 (PLC) and Hep3B. Gossypol treatment at a concentration ≥ 10 μM for 48 h significantly inhibited the viability of PLC and Hep3B cells (Figure 1A). The colony formation assay also reflects cell viability; hence, we further evaluated the inhibitory effect of gossypol on HCC colony formation. As shown in Figure 1B, gossypol inhibited colony formation in PLC and Hep3B cells in a dose-dependent manner. Since gossypol showed significant cytotoxic effects on HCC cells, we next carried out experiments using annexin V/PI staining to assess this type of cell death. PLC and Hep3B cells underwent apoptosis when treated with gossypol (Figure 1C). Quantitative analysis with flow cytometry showed that nearly 70% of cells underwent early- or late-stage apoptosis after treatment with 20 μM gossypol for 48 h. We further examined intrinsic apoptosis pathway-related proteins by western blot analysis. The results showed that gossypol induced cleaved caspase-9, caspase-3, and poly ADP ribose polymerase (PARP) in HCC cells in a time- and dose-dependent manner, indicating that intrinsic apoptosis was activated in these cells by gossypol treatment (Figure 1D).

Ultrastructural examinations show a dilated ER and autophagosomes in gossypol-treated HCC cells. Although gossypol was confirmed to induce cell death in HCC cells primarily through apoptosis, the specific mechanism by which the intrinsic apoptotic signaling pathway is triggered by gossypol to induce apoptosis in HCC cells remains unknown. Hence, we examined the ultrastructure of gossypol-treated cells using TEM (Figure 2). The mitochondria and ER of HCC cells were normal in the control group (0 μM gossypol-treated group), whereas the mitochondria had a "fuzzy" appearance and the ER was significantly dilated in the 10 μM gossypol-treated group. Additionally, autophagosomes were visible in HCC cells after gossypol treatment. These phenomena indicated that gossypol induces ER stress and autophagy in HCC cells.

Gossypol induces ER stress in HCC cells. The ER plays a critical role in Ca^{2+} homeostasis, and an aberrant distribution of Ca^{2+} could, to a certain extent, indicate ER stress in cells. After treatment with 20 μM gossypol, the cytoplasmic calcium level reached nearly 10 times that of the control group (0 μM gossypol) (Figure 3A). To confirm the presence of ER stress in gossypol-treated HCC cells, we conducted western blotting experiments to detect ER stress-related proteins. As the downstream molecules of the UPR pathway, CHOP, phosphorylated eIF2α and IRE-1α were significantly up-regulated following gossypol treatment in a dose-dependent manner (Figure 3B). Nevertheless, the expression of the chaperone protein binding immunoglobulin protein (BiP) was barely affected in HCC cells. The typical ER stress inducer tunicamycin was used as a positive control (Figure 3B). Thus, gossypol induces ER stress in HCC cells, which might lead to the activation of the apoptotic pathway.

CHOP is a key factor in gossypol-induced cell death. As CHOP was significantly activated during gossypol-induced ER stress in HCC cells (Figure 4A, in the negative control [NC] group), we utilized siRNA targeting CHOP (si-CHOP) to study the specific role of this protein. si-CHOP transfection significantly attenuated gossypol-induced CHOP accumulation in the si-CHOP group (Figure 4A). PARP was obviously cleaved following gossypol treatment in the NC group, whereas little PARP cleavage was observed after CHOP was knocked down by siRNA transfection in the si-CHOP group. We next examined the cytotoxic effect of gossypol on HCC cells following CHOP knockdown (si-CHOP). The CCK-8 assay showed that the cytotoxic effect of gossypol was partially abolished when CHOP was knocked down (Figure 4D, si-CHOP group). At the same time, we also examined the function of IRE-1α and phosphorylated eIF2α in the same way. The results showed that IRE-1α or phosphorylated eIF2α knockdown led to the opposite effect, in which cells exhibited increased sensitivity to gossypol (Figure 4B, C, D, si-IRE-1α and phosphorylated eIF2α). These results indicated that CHOP plays a key role in gossypol-induced apoptosis, whereas the accumulation of IRE-1α and phosphorylated eIF2α plays a protective role.

Autophagy protects HCC cells from apoptosis. The autophagosomes that were observed in gossypol-treated cells via TEM are an indicator of autophagy (Figure 2). We then investigated the role of gossypol-induced autophagy in the gossypol-induced apoptotic process. LC3-I was converted into LC-3II in a dose-dependent manner in PLC and Hep3B cells treated with gossypol, indicating dose-dependent autophagic activity (Figure 5A). ATG5 is an important regulator of autophagy, and we utilized a siRNA that targeted this regulator to block autophagy in HCC cells. As a result, when ATG5 was knocked down, gossypol-induced LC3 conversion was partially inhibited. At the same time, once ATG5 was knocked down, PARP cleavage was increased following gossypol treatment (Figure 5B). The CCK-8 assay showed that ATG5 knocked down could enhance the cytotoxic effect of gossypol (Figure 5C). Our results demonstrated that gossypol-induced autophagy plays a protective role in the gossypol-induced apoptotic process. Inhibition of autophagy by RNA interference enhanced apoptosis of HCC cells during gossypol treatment. This induction of autophagy is a typical feedback mechanism that cells utilize to protect themselves.

An autophagy inhibitor enhances the anti-HCC effect of gossypol *in vivo*. We generated a

tumor orthotopic xenograft model to investigate the anti-HCC effect and toxicity of gossypol on normal tissues/hepatocytes *in vivo*. Gossypol significantly inhibited tumor volume compared to that of the control and CQ groups, and gossypol combined with CQ further reduced tumor volume (Figure 6A). Ki67, a marker of proliferation, showed weak staining in the gossypol and CQ combined treatment group (GOS+CQ group), whereas TUNEL staining for apoptosis was most robust in the GOS+CQ group (Figure 6B, C). CHOP was also stained in the tumor tissues, and GOS+CQ group increased CHOP expression in HCC tissues (Figure 6D). The level of cleaved caspase-3 was higher in the gossypol and GOS+CQ groups, which indicated that more cells died (Figure 6E).

Gossypol is a hepatotoxic substance, so we verified the safety of the gossypol concentration used in our experiment. The viability of primary hepatocytes was nearly 90% when treated with 20 μM gossypol and 86% with 20 μM gossypol plus 20 μM CQ (Figure 6F). Furthermore, H&E staining of normal liver, lung, heart, kidney and spleen tissues indicated barely any difference between the groups (Figure 6G, S1).

These results were in accordance with the *in vitro* studies, showing that gossypol inhibited HCC cell viability and that the inhibition of autophagy enhanced this effect.

Discussion

Gossypol is a naturally occurring polyphenol that has been used as a male contraceptive. The biological activity of this compound has recently been exploited for its anticancer potential [14]. In fact, several studies have shown that gossypol influences cell survival in different cancers, including HCC [15, 18, 26]. In the present study, we verified the anti-tumor effect of gossypol on two HCC cell lines. Our results were in accordance with previous studies, showing that gossypol induced distinct cytotoxicity in HCC cells.

Although it is accepted that gossypol inhibits the proliferation of different cancer cells, the specific mechanism underlying its anti-HCC effect remains elusive. Many previous studies have regarded gossypol as a BH3 mimetic [18]. More specifically, gossypol inhibits proliferation of cancer cells through the induction of apoptosis, which is achieved via the inhibition of Bcl-2 and Bcl-xl [17, 18]. Oliver et al. reported that gossypol acts directly on mitochondria to induce cell death [20]. The ability of gossypol to induce intrinsic apoptosis was also verified in our experiments.

Death receptors, mitochondria, and ER stress are three common pathways for the induction of apoptosis [10]. The normal ER lumen promotes proper protein folding, but under stress conditions, the ER cannot meet the demands for protein folding. Misfolded proteins accumulate, and an adaptive UPR is activated to restore ER homeostasis. When the stress is strong and persistent, the UPR eventually induces apoptosis via mitochondria. Studies have reported numerous anticancer agents that target the ER stress pathway. In their latest study, Zhang et al. discovered a new synthetic flavonoid that activates the extrinsic apoptotic pathway in human lung cancer cells via ER stress [27]. Lu et al. identified a new anti-colorectal cancer agent, cinobufagin. The specific mechanism of this anticancer drug is the activation of ER stress-related apoptosis [28]. Moreover, several existing anticancer drugs have been found to induce ER stress. Sorafenib is an oral multikinase inhibitor that has inhibitory effects on HCC cells. Shi et al. showed that sorafenib induces apoptosis in HCC cells by inducing ER stress. Additionally, they found that sorafenib induces ER stress-related apoptosis independently of the MEK1/2-ERK1/2 pathway and

that knockdown of a key ER stress regulator attenuates its anti-HCC effect [29]. Soderquist et al. reported that ER stress in cancer cells could be triggered by gossypol, and this study illustrated a new potential application for the anticancer action of gossypol [19].

In the present study, we observed the ultrastructure of gossypol-treated cells via TEM and found that abundant vacuoles appeared in HCC cells, which were, more accurately, enlarged ER. Meanwhile, CHOP, phosphorylated eIF2α and IRE-1α accumulated with increasing treatment time or dose. The accumulation of these factors is a typical sign of ER stress-dependent UPR signaling [30]. Disequilibrium of calcium homeostasis is another sign of ER stress, as ER homeostasis is critical for the maintenance of cytosolic calcium levels [8].

CHOP and IRE-1α are key regulators during ER stress; however, these two proteins play different roles in cell fate. To date, whether the function of IRE-1α is proapoptotic or pro-survival remains unclear. Urano et al. [31] showed that IRE-1α activates ASK1/JNK to promote cell death. Ghosh et al. demonstrated that IRE-1α inhibition preserves survival in models of ER stress-induced diseases [32]. However, IRE-1α-mediated RNA decay can also inhibit some proapoptotic proteins, which further promotes cell survival. For example, Lu et al. found that IRE-1α inhibits the TNF-related apoptosis-inducing ligand receptor 2 and protects cells from apoptosis [33]. Unlike IRE-1α or phosphorylated eIF2α, CHOP has been shown to play a critical role in cell death. Studies have revealed that CHOP induces proapoptotic proteins and inhibits pro-survival proteins [34].

In our study, we found that knocking down CHOP expression with siRNA minimized the anti-HCC effect of gossypol, which indicated that CHOP plays a critical role in the induction of apoptosis. However, phosphorylated eIF2α or IRE-1α inhibition led to the opposite effect. Briefly, gossypol promoted ER stress in HCC cells, and CHOP was the key factor that induced apoptosis, whereas phosphorylated eIF2α and IRE-1α played a protective role.

As mentioned previously, autophagy is often accompanied with ER stress. The UPR activated during ER stress and the major ER stress pathway stimulates autophagy, which plays a dual role in affecting cell fate [12, 35]. In our study, we observed the conversion of LC3-I to LC3-II, which reflects the activation of autophagy. To determine the effect of autophagy induced by gossypol, we knocked down the key regulators of autophagy ATG5 using siRNA. Apoptosis of HCC cells increased once autophagy was inhibited. Our results indicated that autophagy protected the cells from ER-related apoptosis. Then, using *in vivo* experiments, we established the anti-HCC effect of gossypol. Since autophagy plays a protective role, we combined the specific autophagy inhibitor CQ with gossypol to inhibit the growth of *in situ* tumors. The results were consistent with the *in vitro* assays, showing that inhibition of autophagy enhanced the anti-HCC effect of gossypol.

Conclusion

In summary, our study showed that gossypol induced apoptosis in HCC cells via ER stress and that the autophagy that occurred with ER stress had a protective effect. Gossypol may become a new therapeutic strategy for HCC, and combination therapy with an autophagy inhibitor may enhance the anti-HCC effect of gossypol.

Authors' contributions

Conceived and designed the experiments: CP Jiang, JH Wu, ZX Wang, G Zhang. Performed the

experiments: G Zhang, ZX Wang, WB Chen, Y Cao, JY Wu, GH Qiang, AL Ji. Analyzed the data: G Zhang, ZX Wang, CP Jiang, JH Wu. Contributed reagents, materials, and funds: CP Jiang, JH Wu, ZX Wang, WB Chen. Wrote the paper: G Zhang, JH Wu

Funding

The research was supported by the National Natural Science Foundation of China (no. 81572393, 81602093), Key Project supported by the Medical Science and Technology Development Foundation, Nanjing Municipality Health Bureau (no. ZKX15020, ZKX17022), the Natural Science Foundation of Jiangsu Province (no. BK20160118 and BK20141324), and the Fundamental Research Funds for the Central Universities (no. 021414380215, 021414380242, 021414380258, 14380329/3), and the Primary Research & Development Plan of Jiangsu Province (BE2018701).

Conflict of interest

The authors declare no conflict of interest.

Acknowledgments

We thank the Translational Medicine Core Facilities of the Medical School of Nanjing University for instrument support.

References

1. Torre, L.A., Bray, F., Siegel, R.L., Ferlay, J., Lortet-Tieulent, J., Jemal, A., 2015. Global cancer statistics, 2012. CA: a cancer journal for clinicians 65(2), 87-108.

2. Forner, A., Llovet, J.M., Bruix, J., 2012. Hepatocellular carcinoma. Lancet 379(9822), 1245-1255.

3. Villanueva, A., Hernandez-Gea, V., Llovet, J.M., 2013. Medical therapies for hepatocellular carcinoma: a critical view of the evidence. Nature reviews. Gastroenterology & hepatology 10(1), 34-42.

4. Bruix, J., Sherman, M., American Association for the Study of Liver, D., 2011. Management of hepatocellular carcinoma: an update. Hepatology 53(3), 1020-1022.

5. Pistritto, G., Trisciuoglio, D., Ceci, C., Garufi, A., D'Orazi, G., 2016. Apoptosis as anticancer mechanism: function and dysfunction of its modulators and targeted therapeutic strategies. Aging 8(4), 603-619.

6. Liu, Z., Lv, Y., Zhao, N., Guan, G., Wang, J., 2015. Protein kinase R-like ER kinase and its role in endoplasmic reticulum stress-decided cell fate. Cell death & disease 6, e1822.

7. Kupsco, A., Schlenk, D., 2015. Oxidative stress, unfolded protein response, and apoptosis in developmental toxicity. International review of cell and molecular biology 317, 1-66.

8. Krebs, J., Agellon, L.B., Michalak, M., 2015. Ca(2+) homeostasis and endoplasmic reticulum (ER) stress: An integrated view of calcium signaling. Biochemical and biophysical research communications 460(1), 114-121.

9. Xu, C., Bailly-Maitre, B., Reed, J.C., 2005. Endoplasmic reticulum stress: cell life and death decisions. The Journal of clinical investigation 115(10), 2656-2664.

10. Ryoo, H.D., 2016. Long and short (timeframe) of endoplasmic reticulum stress-induced cell death. The FEBS journal 283(20), 3718-3722.

11. Su, J., Zhou, L., Kong, X., Yang, X., Xiang, X., Zhang, Y., Li, X., Sun, L., 2013. Endoplasmic reticulum is at the crossroads of autophagy, inflammation, and apoptosis signaling pathways and participates in the pathogenesis of diabetes mellitus. Journal of diabetes research 2013, 193461.

12. Ondrej, M., Cechakova, L., Durisova, K., Pejchal, J., Tichy, A., 2016. To live or let die: Unclear task of autophagy in the radiosensitization battle. Radiotherapy and oncology : journal of the European Society for Therapeutic Radiology and Oncology 119(2), 265-275.

13. Wang, Z., Jiang, C., Chen, W., Zhang, G., Luo, D., Cao, Y., Wu, J., Ding, Y., Liu, B., 2014. Baicalein induces apoptosis and autophagy via endoplasmic reticulum stress in hepatocellular carcinoma cells. BioMed research international 2014, 732516.

14. Sung, B., Ravindran, J., Prasad, S., Pandey, M.K., Aggarwal, B.B., 2016. Gossypol induces death receptor-5 through activation of ROS-ERK-CHOP pathway and sensitizes colon cancer cells to TRAIL. The Journal of biological chemistry 291(32), 16923.

15. Wang, B., Chen, L., Ni, Z., Dai, X., Qin, L., Wu, Y., Li, X., Xu, L., Lian, J., He, F., 2014. Hsp90 inhibitor 17-AAG sensitizes Bcl-2 inhibitor (-)-gossypol by suppressing ERK-mediated protective autophagy and Mcl-1 accumulation in hepatocellular carcinoma cells. Experimental cell research 328(2), 379-387.

16. Wu, Y., Wei, Y.N., Yue, W.Y., Chen, W.F., Fu, S., 2015. Influence of gossypol acetic acid on the growth of human adenoid cystic carcinoma ACC-M cells and the expression of DNA methyltransferase 1. Genetics and molecular research : GMR 14(4), 13456-13466.

17. Baoleri, X., Dong, C., Zhou, Y., Zhang, Z., Lu, X., Xie, P., Li, Y., 2015. Combination of L-gossypol and low-concentration doxorubicin induces apoptosis in human synovial sarcoma cells. Molecular medicine reports 12(4), 5924-5932.

18. Zhao, G.X., Xu, L.H., Pan, H., Lin, Q.R., Huang, M.Y., Cai, J.Y., Ouyang, D.Y., He, X.H., 2015. The BH3-mimetic gossypol and noncytotoxic doses of valproic acid induce apoptosis by suppressing cyclin-A2/Akt/FOXO3a signaling. Oncotarget 6(36), 38952-38966.

19. Soderquist, R.S., Danilov, A.V., Eastman, A., 2014. Gossypol increases expression of the pro-apoptotic BH3-only protein NOXA through a novel mechanism involving phospholipase A2, cytoplasmic calcium, and endoplasmic reticulum stress. The Journal of biological chemistry 289(23), 16190-16199.

20. Oliver, C.L., Miranda, M.B., Shangary, S., Land, S., Wang, S., Johnson, D.E., 2005. (-)-Gossypol acts directly on the mitochondria to overcome Bcl-2- and Bcl-X(L)-mediated apoptosis resistance. Molecular cancer therapeutics 4(1), 23-31.

21. Teng, C.S., 1995. Gossypol-induced apoptotic DNA fragmentation correlates with inhibited protein kinase C activity in spermatocytes. Contraception 52(6), 389-395.

22. Mani, J., Vallo, S., Rakel, S., Antonietti, P., Gessler, F., Blaheta, R., Bartsch, G., Michaelis, M., Cinatl, J., Haferkamp, A., Kogel, D., 2015. Chemoresistance is associated with increased cytoprotective autophagy and diminished apoptosis in bladder cancer cells treated with the BH3 mimetic (-)-Gossypol (AT-101). BMC cancer 15, 224.

23. Gao, P., Bauvy, C., Souquere, S., Tonelli, G., Liu, L., Zhu, Y., Qiao, Z., Bakula, D., Proikas-Cezanne, T., Pierron, G., Codogno, P., Chen, Q., Mehrpour, M., 2010. The Bcl-2 homology domain 3 mimetic gossypol induces both Beclin 1-dependent and Beclin 1-independent cytoprotective autophagy in cancer cells. The Journal of biological chemistry 285(33), 25570-25581.

24. Jang, G.H., Lee, M., 2014. BH3-mimetic gossypol-induced autophagic cell death in mutant BRAF melanoma cells with high expression of p21Cip(1).). Life sciences 102(1), 41-48.

25. Liu, X.H., Yang, Y.F., Fang, H.Y., Wang, X.H., Zhang, M.F., Wu, D.C., 2017. CEP131 indicates poor prognosis and promotes cell proliferation and migration in hepatocellular carcinoma. The international journal of biochemistry & cell biology 90, 1-8.

26. Xiong, J., Li, J., Yang, Q., Wang, J., Su, T., Zhou, S., 2017. Gossypol has anti-cancer effects by dual-targeting MDM2 and VEGF in human breast cancer. Breast cancer research : BCR 19(1), 27.

27. Zhang, Y., Xu, X., Li, W., Miao, H., Huang, S., Zhou, Y., Sun, Y., Li, Z., Guo, Q., Zhao, L., 2016. Activation of endoplasmic reticulum stress and the extrinsic apoptotic pathway in human lung cancer cells by the new synthetic flavonoid, LZ-205. Oncotarget 7(52), 87257-87270.

28. Lu, X.S., Qiao, Y.B., Li, Y., Yang, B., Chen, M.B., Xing, C.G., 2017. Preclinical study of cinobufagin as a promising anti-colorectal cancer agent. Oncotarget 8(1), 988-998.

29. Shi, Y.H., Ding, Z.B., Zhou, J., Hui, B., Shi, G.M., Ke, A.W., Wang, X.Y., Dai, Z., Peng, Y.F., Gu, C.Y., Qiu, S.J., Fan, J., 2011. Targeting autophagy enhances sorafenib lethality for hepatocellular carcinoma via ER stress-related apoptosis. Autophagy 7(10), 1159-1172.

30. Hiramatsu, N., Chiang, W.C., Kurt, T.D., Sigurdson, C.J., Lin, J.H., 2015. Multiple Mechanisms of Unfolded Protein Response-Induced Cell Death. The American journal of pathology 185(7), 1800-1808.

31. Urano, F., Wang, X., Bertolotti, A., Zhang, Y., Chung, P., Harding, H.P., Ron, D., 2000. Coupling of stress in the ER to activation of JNK protein kinases by transmembrane protein kinase IRE1. Science 287(5453), 664-666.

32. Ghosh, R., Wang, L., Wang, E.S., Perera, B.G., Igbaria, A., Morita, S., Prado, K., Thamsen, M., Caswell, D., Macias, H., Weiberth, K.F., Gliedt, M.J., Alavi, M.V., Hari, S.B., Mitra, A.K., Bhhatarai, B., Schurer, S.C., Snapp, E.L., Gould, D.B., German, M.S., Backes, B.J., Maly, D.J., Oakes, S.A., Papa, F.R., 2014. Allosteric inhibition of the IRE1alpha RNase preserves cell viability and function during endoplasmic reticulum stress. Cell 158(3), 534-548.

33. Lu, M., Lawrence, D.A., Marsters, S., Acosta-Alvear, D., Kimmig, P., Mendez, A.S., Paton, A.W., Paton, J.C., Walter, P., Ashkenazi, A., 2014. Opposing unfolded-protein-response signals converge on death receptor 5 to control apoptosis. Science 345(6192), 98-101.

34. Ohoka, N., Yoshii, S., Hattori, T., Onozaki, K., Hayashi, H., 2005. TRB3, a novel ER stress-inducible gene, is induced via ATF4-CHOP pathway and is involved in cell death. The EMBO journal 24(6), 1243-1255.

35. Kroemer, G., Marino, G., Levine, B., 2010. Autophagy and the integrated stress response. Molecular cell 40(2), 280-293.

Figure legends

Figure 1. Gossypol induces apoptosis in HCC cells. **A.** PLC and Hep3B cells were treated with increasing concentrations of gossypol for 48 h. Cell viability was measured using the CCK-8 assay. Data are expressed as the mean ± SD. *P < 0.05, **P < 0.01, and ***P < 0.001 compared with the 0 μM group. **B.** Cell colonies were stained by crystal violet. The number of colonies was counted and normalized to controls (0 μM gossypol group). *P < 0.05, **P < 0.01, and ***P < 0.001 compared with the 0 μM group. This result is representative for two independent replicates. **C.** HCC cells were stained with annexin V/PI. Gossypol-induced cell death was verified by flow cytometry. This result is representative for two independent replicates. **D.** PLC and Hep3B cells were treated with gossypol at the indicated concentrations for 48h or treated with 20 μM gossypol for the indicated times. The apoptosis-related proteins caspase-3, caspase-9, and PARP together with their cleaved forms were analyzed by western blotting. GAPDH was used as a loading control. This result is representative for three independent replicates.

Figure 2. Gossypol induces ultrastructural changes. Ultrastructural changes were observed by TEM in PLC and Hep3B cells after treatment with the indicated concentrations of gossypol for 48 h. Arrows indicate normal ER, asterisks indicate dilated ER, and arrowheads show autophagosomes. This result is representative for two independent replicates.

Figure 3. Gossypol induces ER stress in HCC cells. **A.** PLC and Hep3B cells were treated with gossypol at the indicated concentration for 48 h, and the cells were loaded with Fluo-3 AM. Cytosolic calcium was measured by flow cytometry. This result is representative for two independent replicates. **B.** PLC and Hep3B cells were treated with gossypol at the indicated concentration for 48 h. ER stress pathway-related proteins were measured by western blotting. GAPDH was used as a loading control, and cells treated with tunicamycin (TM, 5 μg/mL) for 6 h were regarded as the positive ER stress group. This result is representative for three independent replicates.

Figure 4. ER stress-related proteins play diverse roles in gossypol-induced apoptosis. **A.** The cells were transfected with CHOP siRNA before treatment with 0, 10, or 20 μM gossypol for 48 h. Cleaved PARP levels were determined by western blotting. This result is representative for three independent replicates. **B.** PLC and Hep3B cells were transfected with IRE-1α siRNA before treatment with 0, 10, or 20 μM gossypol for 48 h. Cleaved PARP levels were determined by western blotting. This result is representative for three independent replicates. **C.** The cells were transfected with eIF2α siRNA before treatment with 0, 10, or 20 μM gossypol for 48 h. Cleaved PARP levels were determined by western blotting. This result is representative for three independent replicates. **D.** Hep3B/PLC cells were transfected with CHOP, IRE-1α, eIF2α or NC siRNA before treatment with 0, 2.5, 5, 10, or 20 μM gossypol for 48 h. The viability of Hep3B/PLC cells following CHOP, IRE-1α, eIF2α and NC siRNA transfection was determined using the CCK-8 assay. Data are expressed as the mean ± SD. *P < 0.05, **P < 0.01, and ***P < 0.001 compared with the corresponding NC group.

Figure 5. Initiation of protective autophagy in HCC cells. **A.** PLC/Hep3B cells were treated with

various concentrations of gossypol. The protein level of LC3 was determined by western blotting. This result is representative for three independent replicates. **B.** PLC/Hep3B cells were transfected with ATG5 siRNA (si-ATG5) and treated with 0, 10, or 20 μM gossypol for 48 h. Cleaved PARP and ATG5 levels were determined by western blotting. GAPDH was used as a loading control. This result is representative for three independent replicates. **C.** Hep3B/PLC cells were treated with 0, 2.5, 5, 10, or 20 μM gossypol with or without si-ATG5 for 48 h. The viability of cells was determined using the CCK-8 assay. Data are expressed as the mean ± SD. *P < 0.05, **P < 0.01, and ***P < 0.001 compared with the corresponding NC group.

Figure 6. Gossypol inhibits tumor growth *in vivo*. **A.** An *in situ* HCC model was generated by the orthotopic injection of PLC cells. At 1 week after injection, the indicated drugs were administered by gavage daily until the mice were sacrificed. Mice in the NC group were administered water, mice in the CQ group were administered 60 mg/kg/day CQ, mice in the GOS group were administered 10 mg/kg/day gossypol, and mice in the CQ+GOS group were administered 60 mg/kg/day CQ and 10 mg/kg/day gossypol. Tumor volumes were measured. **B, C, D.** Ki67 **(B)** and TUNEL **(C)** staining indicated proliferation and apoptosis in the tumor tissues, respectively. CHOP accumulation in tumor tissue was also detected via IHC **(D)** (scale bar, 25 μm). Staining intensity levels from the IHC experiment were analyzed and normalized to the control groups. *P < 0.05, **P < 0.01, and ***P < 0.01 compared with the corresponding NC groups. **E.** Proteins were isolated from the tumor tissues for electrophoresis. Caspase-3 and cleaved caspase-3 levels were detected via western blotting. GAPDH was used as a loading control. **F.** Primary hepatocytes were isolated from healthy mice liver and the cells were treated with increasing concentrations of gossypol with or without CQ for 48 h. Cell viability was measured using the CCK-8 assay. *P < 0.05, **P < 0.01, and ***P < 0.001 compared with the 0 μM group. **G.** H&E staining of normal liver tissue indicated the toxicity of gossypol (scale bar, 25 μm). Representative staining images were shown. Tissue staining performed on 5 samples from each group.

Figures

Figure 1

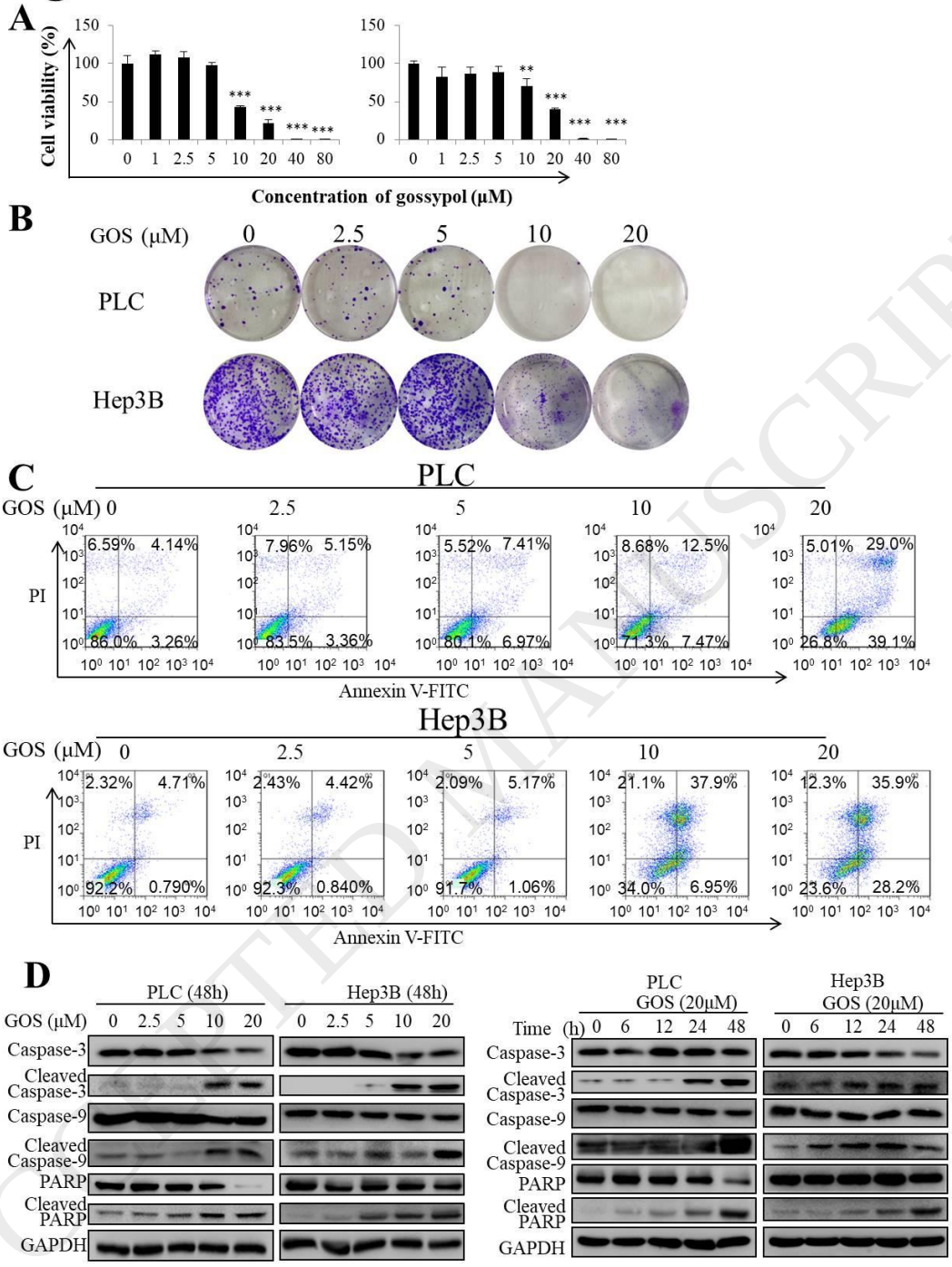

Figure 2

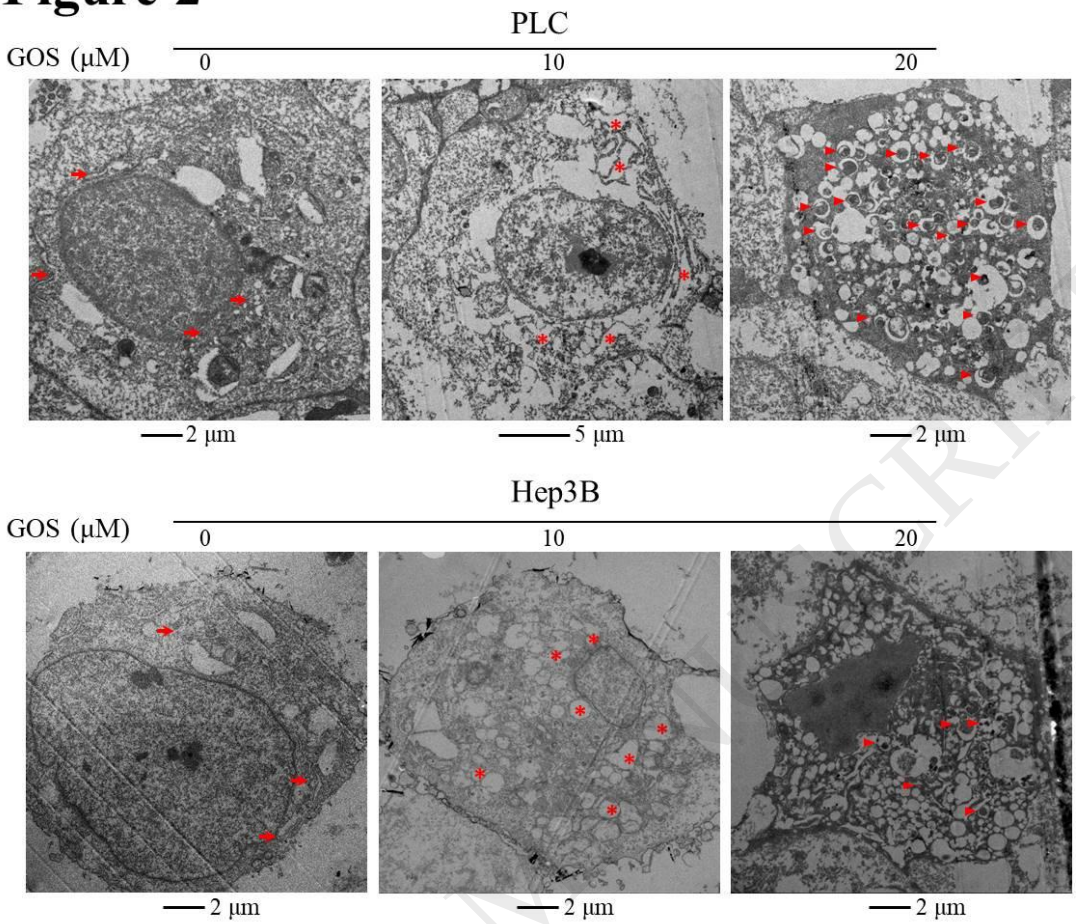

Figure 3

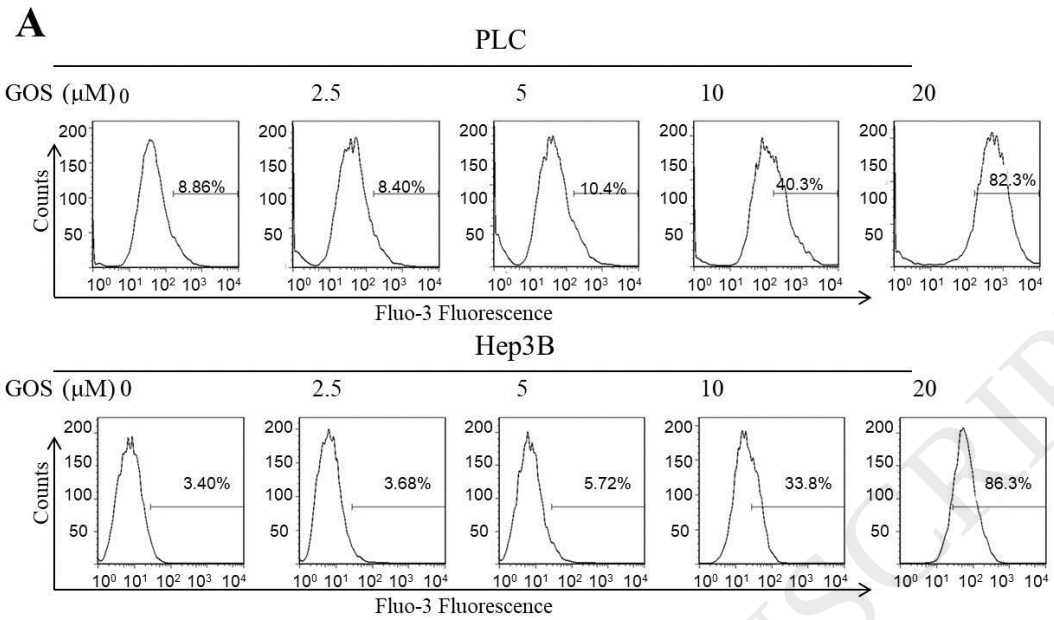

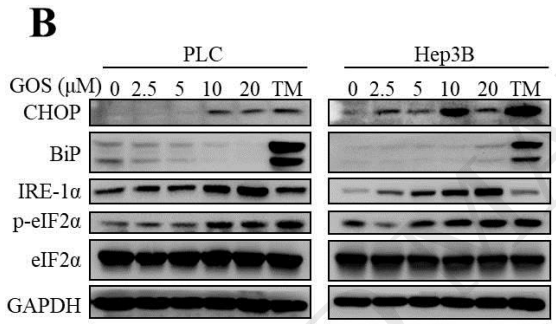

Figure 4

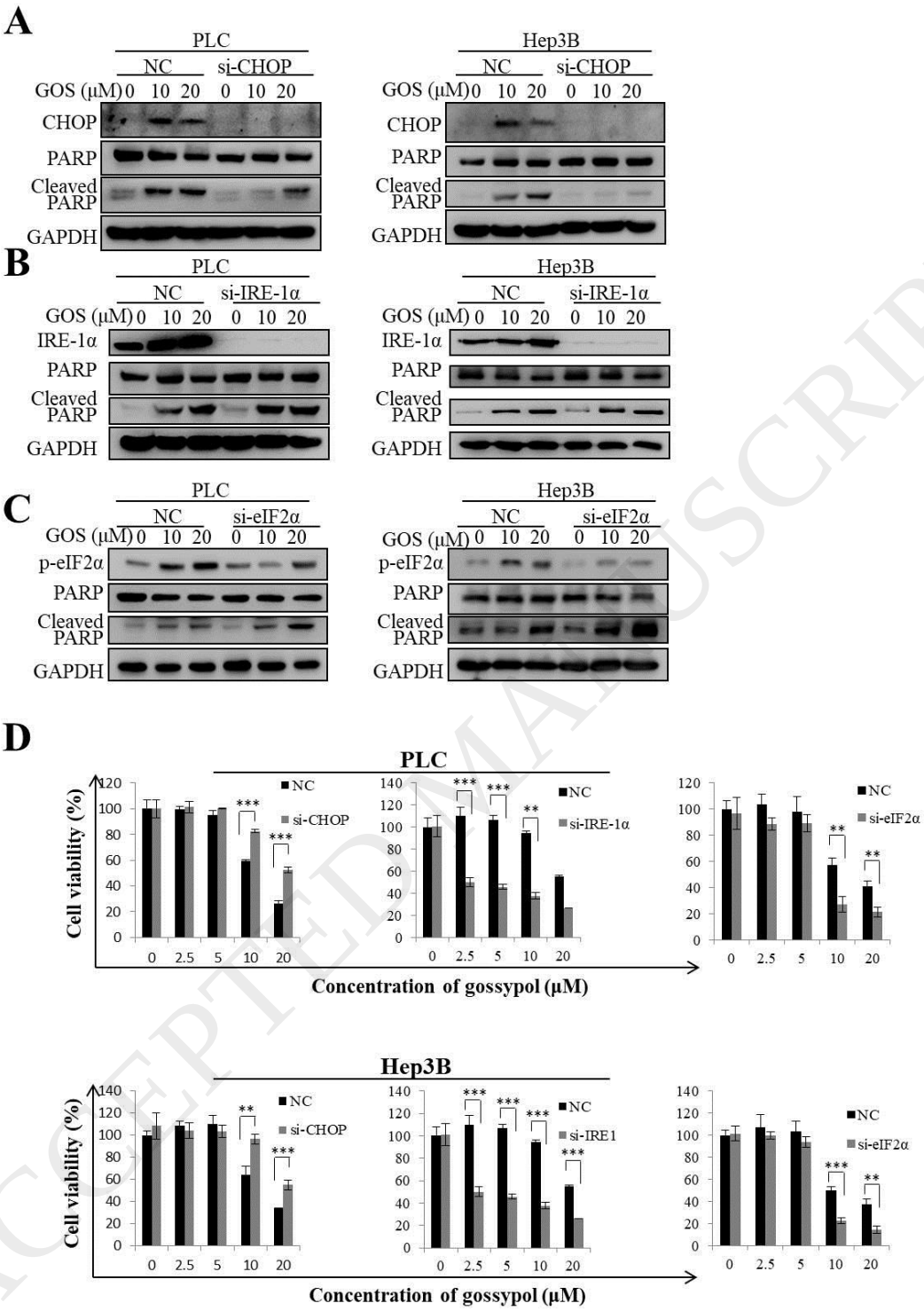

Figure 5

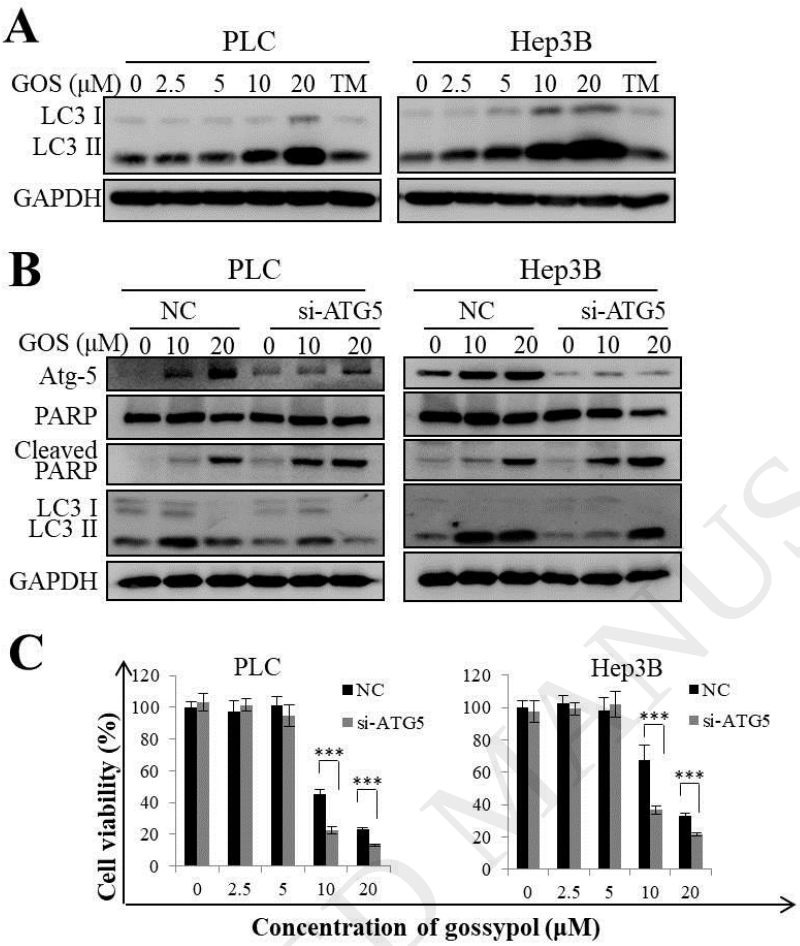

Figure 6